

Suffusion susceptibility characterization by triaxial erodimeter and statistical analysis

V.T. Le, D. Marot

Nantes Université, Institut de Recherche en Génie Civil et Mécanique, GeM, France

A. Rochim,

Nantes Université, Institut de Recherche en Génie Civil et Mécanique, GeM, France

Sultan Agung Islamic University, Civil Engineering Department, Indonesia

F. Bendahmane

Nantes Université, Institut de Recherche en Génie Civil et Mécanique, GeM, France

H.H. Nguyen,

University of Science and Technology-The University of Danang, Vietnam

ABSTRACT: Suffusion process corresponds to the coupled processes of detachment-transport-filtration of the soil's fine fraction within the voids between the coarse fraction. Because of the great length of earth structures and because of the heterogeneities of soils, it is very difficult to characterize the suffusion susceptibility of soils all along the earth structures. So, a statistical analysis can be performed in order to optimize the experimental campaign. By using a specific triaxial erodimeter, an experimental program was setup to study suffusion susceptibility of thirty two specimens. The suffusion susceptibility is determined by the erosion resistance index. Ten physical parameters are determined and a statistical analysis is performed in order to identify the main parameters for a correlation with erosion resistance index. The multivariate statistical analysis leads to an expression of the erosion resistance index as a function of eight physical parameters, and by distinguishing the gap-graded and widely-graded soils, another new correlation is obtained with five physical parameters.

1 INTRODUCTION

Fell & Fry (2013) distinguished four types of internal erosion: concentrated leak erosion, backward erosion, contact erosion and suffusion. Concentrated leak erosion may occur through a crack or hydraulic fracture. Backward erosion mobilizes all the grains in regressive way (i.e. from the downstream part of earth structure to the upstream part) and includes backward erosion piping and global backward erosion. Contact erosion occurs where a coarse soil is in contact with a fine soil. The phenomenon of suffusion corresponds to the process of detachment and then transport of the finest particles within the porous network.

For the first three aforementioned processes of internal erosion, different classifications exist in order to evaluate the soil erodibility, whereas in the case of suffusion, only one susceptibility classification is available and recently proposed by Marot et al. (2016). The absence of several suffusion susceptibility classifications may be due to the complexity of this process, which appears as the result of the coupled processes: detachment – transport – filtration of a part of the finest fraction within the porous network. For this classification, the cumulative energy expended by the seepage flow is computed and the induced erosion is evaluated by the cumulative loss dry mass. Six categories of soil erodibility are proposed from very resistant to very erodible.

Soils which compose hydraulic earth structures and their foundations (for example: 8000 km of dikes in France and 13200 km of dikes in Vietnam) are characterized by great heterogeneities. In consequence, statistical analysis can be useful in order to optimize the experimental campaign for taking into account these heterogeneities and then, the possible wide range of soil erodibility.

This paper deals with the relationship between suffusion susceptibility and other soil properties. By using a dedicated erodimeter, the erodibility is evaluated for fourteen soils. These results are interpreted by the energy method and a statistical analysis, performed with Xlstat software shows a new correlation of the erosion resistance index with several physical parameters.

2 IDENTIFICATION OF PREDOMINANT PARAMETERS

Lafleur et al. (1989) described the key influence of the grain size distribution on the suffusion process and they distinguished three main gradation curves: linear distribution, discontinuous distribution and upwardly concave distribution. The concave distribution consists of a poorly graded coarse fraction associated to a highly graded fine fraction. The soils that are likely to suffer from suffusion are, according to Fell & Fry (2007) “internally unstable”, i.e. their

grain-size distribution curve is either discontinuous or upwardly concave. Based on this information, several criteria have been proposed in literature, and recently Chang & Zhang (2013) proposed three categories of soil erodability from the comparison of criteria of Istonima, Kézdi and Kenney & Lau. They defined P as the mass fraction of particles finer than 0.063mm. For gap-graded soil, Chang & Zhang defined the gap ratio as: $G_r = d_{max}/d_{min}$ (d_{max} and d_{min} : maximal and minimal particle sizes characterizing the gap in the grading curve). For P less than 10%, the authors assumed that the stability is correctly assessed using the criterion $G_r < 3$. For P higher than 35%, the gap graded soil is reputed stable, and with P in the range 10% to 35% the soil is stable if $G_r < 0.3P$. According to Chang & Zhang, their method is only applicable to low plasticity soils.

By using a triaxial erodimeter, Marot et al. (2012) determined the suffusion susceptibility of three mixtures of kaolin and aggregates. The results indicate that suffusion process depends on the grain angularity of coarse fraction. With a same grain size distribution, angularity of coarse fraction grains contributes to increase the suffusion resistance. Thus the parameter of shape of grains plays also an important role on suffusion susceptibility.

The physicochemical characteristics of the fluid and solid phases are also crucial, particularly in the case of cohesive soils. For the same type of clay, several tests performed in clayey sands have shown that suffusion decreases with the increase of the clay content (Bendahmane et al. 2008). Arulanandan & Perry (1983) showed that the nature of the clay influences the initiation of the detachment of clay particles. Thus, as any other type of erosion, suffusion, which depends on the conditions of detachment of particles or aggregates of particles, appears to depend on the nature of the clay and for a given type of clay, on the clay percentage.

In addition with material susceptibility, Garner & Fannin (2010) take into account two others main initiation conditions for suffusion: the stress condition and the hydraulic load. For the same material susceptibility, the modification of the effective stress can induce grain rearrangements. Several tests performed in oedometric conditions on unstable soils showed that a rise in the effective stress causes an increase of the soils' resistance to suffusion (Moffat and Fannin 2006). In the same manner, when tests were carried out under isotropic confinement (Bendahmane et al. 2008), the increase in the confinement pressure, and then the increase of soil density allowed a decrease in the suffusion rate.

The hydraulic loading on the grains is often described by three distinct parameters characterizing the hydraulic loading: the hydraulic gradient, the hydraulic shear stress and the pore velocity. The critical values of these three quantities can then be used to characterize the suffusion initiation (Skempton &

Brogan 1994, Moffat & Fannin 2006, Perzmaier 2007 among others). However a fraction of the detached particles can re-settle or be filtered at the bulk of the porous network (Reddi et al. 2000, Bendahmane et al. 2008, Marot et al. 2009, 2011a, Nguyen et al. 2012, Luo et al. 2013). This process can eventually induce local clogging. The processes of detachment, transport and filtration of fine particles are thus inseparable. Therefore, variations of both seepage flow and pressure gradient have to be taken into account to evaluate the hydraulic loading.

3 SUFFUSION SUSCEPTIBILITY CLASSIFICATION

From results of interface erosion tests, Marot et al. (2011b) proposed a new analysis based on the energy expended by the seepage flow which is a function of both the flow rate and the pressure gradient. Three assumptions were used: the fluid temperature is assumed constant, the system is considered as adiabatic and only a steady state is considered. The energy conservation equation permits to express the total flow power as the summation of the power transferred from the fluid to the solid particles and the power dissipated by viscous stresses in the bulk. As the transfer appears negligible in suffusion case (Sibille et al. 2015), the authors suggest to characterize the fluid loading from the total flow power, P_{flow} which is expressed by:

$$P_{flow} = (\gamma_w \Delta z + \Delta P) Q \quad (1)$$

where Q is the fluid flow rate.

$\Delta z > 0$ if the flow is in downward direction, $\Delta z < 0$ if the flow is upward and the erosion power is equal to $Q \Delta P$ if the flow is horizontal.

The expended energy E_{flow} is the time integration of the instantaneous power dissipated by the water seepage for the test duration. For the same duration the cumulative eroded dry mass is determined and the erosion resistance index is expressed by:

$$I_\alpha = -\log \left(\frac{\text{Eroded dry mass}}{E_{flow}} \right) \quad (2)$$

Depending on the values of I_α index, Marot et al. (2016) proposed six categories of suffusion susceptibility from highly erodible to highly resistant (corresponding susceptibility categories: highly erodible for $I_\alpha < 2$; erodible for $2 \leq I_\alpha < 3$; moderately erodible for $3 \leq I_\alpha < 4$; moderately resistant for $4 \leq I_\alpha < 5$; resistant for $5 \leq I_\alpha < 6$; and highly resistant for $I_\alpha \geq 6$).

4 PRINCIPAL COMPONENT ANALYSIS

4.1 Objective and principle of the statistical analysis

At the scale of earth structures, the soil heterogeneities can induce a wide range of soil susceptibility. The characterization of such range needs to perform a large number of erosion tests. In this context, it can be useful to estimate soil erodibility by physical parameters that may be easily measured. The goal of the Principal Component Analysis is to determine the linear correlations between a set of variables. Each variable is represented in a factor space which is equal or less than the number of original variables. The geometrical representation associates a vector to each variable, and the scalar product of two associated vectors is equal to the correlation coefficient of the two parameters. When two variables are far from the center, then, if they are close to each other, they are significantly positively correlated (correlation coefficient r close to 1), if they are orthogonal, they are not correlated (r close to 0), if they are on the opposite side of the center, then they are significantly negatively correlated (r close to -1).

4.2 Multivariate analysis and reduction of parameters

Multivariate analysis allows the full set of variables related to the measurements to be reduced to a subset representing the principal components assuming a linear correlation between the variables. Now by eliminating the variables which are correlated, or seem meaningless by their redundancy information with other variables, a new multivariable analysis can permit to build a correlation with a reduced number of physical parameters.

5 RESULT OF SUFFUSION CHARACTERIZATION

5.1 Specific device

A triaxial erodimeter was designed to apply downward seepage flow on intact soil sample. A detailed description of the device was reported by Bedahmane et al. (2008) and a brief summary is provided hereafter (see Figure 1).

The triaxial erodimeter includes a modified triaxial cell which was designed to saturate the sample in upward direction, to consolidate it under isotropic confinement and finally to force fluid through the sample in downward direction. The system to generate seepage flow under constant hydraulic gradient comprises a pressure sensor and an injection cell connected to air /water interface cylinder. At the

overflow outlet of the effluent tank, water falls in a beaker which is continuously weighed in order to determine injected flow rate. The system to generate seepage flow in flow-rate-controlled conditions comprises a gear pump connected to a pressure sensor at its outlet. For both types of hydraulic loading, the fluid circulates into the top cap which contains a layer of glass beads to diffuse the fluid uniformly on the specimen top surface. The sample is supported by a lower mesh screen of 4 mm opening size in order to allow the migration of all grains. Different wire meshes can be placed on the lower mesh screen in order to take into account the effect of pore opening size on internal erosion (Marot et al. 2009). The funnel – shaped draining system is connected to effluent tank by a glass pipe. The effluent tank is equipped with an overflow outlet (to control the downstream hydraulic head) and a rotating sampling system containing 8 beakers for the sampling of eroded particles carried with the effluent. In the case of clay or silt suffusion, a multi-channel optical sensor is placed around the glass pipe (Marot et al. 2011a). Thanks to a previous calibration, the optical sensor allows measuring the clay or silt concentration within the effluent which is expressed as the ratio of the mass of fine particles to water mass within the fluid. The time integration of the fine particle concentration gives the cumulative eroded dry mass for the corresponding duration (Bendahmane et al. 2008). Moreover, the detection of sand grains in the effluent is assessed from the comparison of the voltages of each LED composing the optical sensor. For a high value of clay or silt concentration within effluent or when effluent contents sand grains, the mass solid measurement can be performed by continuous weighing as mass accuracy of a few milligrams is sufficient.

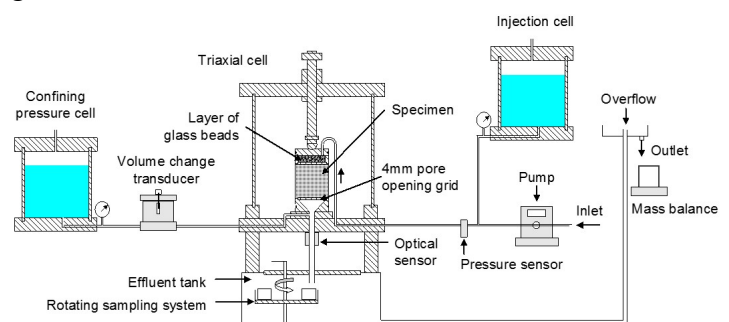


Figure 1. Schematic diagram of the triaxial erodimeter.

A confining pressure cell connected to an air / water interface cylinder is used to generate isotropic confinement. Sample volume change is measured by automatic volume change transducer connected between confining pressure cell and the inlet of triaxial cell.

5.2 Soils properties and physical parameters

Fourteen soils were selected in order to cover a large range of suffusion susceptibility. With this objective, several cohesionless soils but also clayey soils were prepared with gap or widely graded distributions. Four clayey sands were created by the mixture of: Kaolinite Prolabo and Loire sand (soils named K10L90 and K20L80) or Kaolinite Proclay and Fontainebleau sand (named KPr25F75 and KPr20F80). For KPr20F80 soil, specimens were prepared by dynamic compaction with five different values of water content from 4% to 12% (these values are specified in the name of the corresponding specimens). Two soils were the mixtures of sand S1 and gravel G3 (marketed by Sablière Palvadeau, France), soils named DR-A, DR-B, DR-C came from a French dike, and finally two natural soils were sieved with two different values of maximum diameter which is 5 cm and 10 cm for soils CH-5 and CH-10 respectively. A laser diffraction particle-size analyzer was used to measure the grain size distribution of these soils (see Figure 2a and 2b).

Tests were performed with demineralised water and without deflocculation agent.

Table 1 details measured parameters which include the percentage passing of finer such as d_5 , d_{20} , d_{50} , d_{60} , and d_{90} . The percentage P finer than 0.063 mm (Chang & Zhang, 2013) is also mentioned.

For widely graded soils, the fine fraction can be identified within the granular distribution by the minimum value of Kenney and Lau's ratio $(H/F)_{min}$ and the corresponding fine percentage is named *Finer KL*.

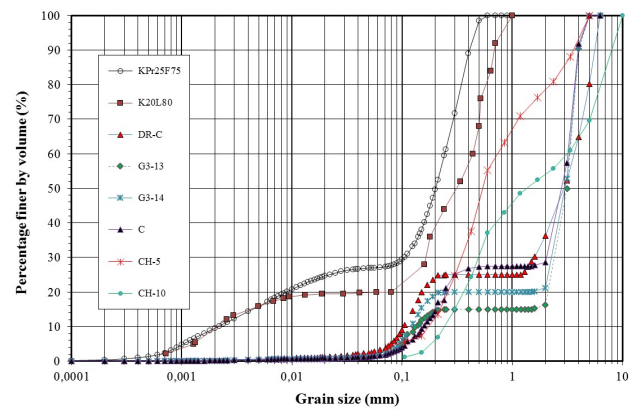
With the objective to take into account the influence of grain shape, internal friction angle ϕ of mixtures was determined thanks to a direct shear stress device.

The blue methylene value V_{BS} permits to highlight the water sensitivity of tested soils, as its value depends on the amount and characteristics of clay minerals present in soil. Based on the V_{BS} value six categories of water sensibility and soil plasticity are proposed by GTR (1992).

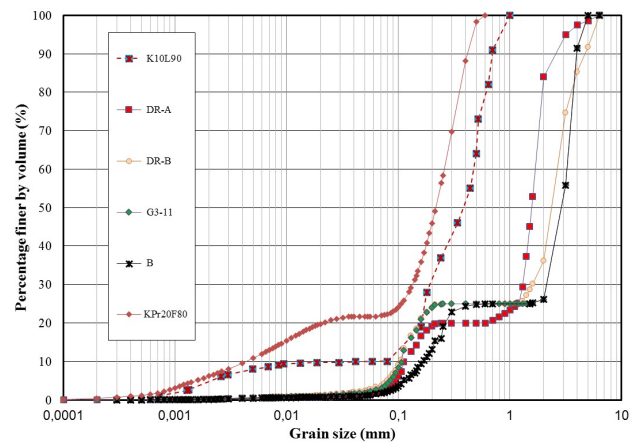
5.3 Test methodology and testing program

Two types of specimen preparation methods were used. For the isotropic confinement condition test (12 tests were performed using such conditions), specimens were prepared using a single layer semi-static compaction technique with a 50 mm diameter and 50 mm high mould. Then, specimens were placed in a membrane and a 15 kPa isotropic confinement pressure was applied. After this step, carbon dioxide was injected followed by the saturation phase which requires approximately 24 h. The last step consists in applying a target value of confining

pressure (between 15 kPa and 200 kPa). Twenty tests were realized without confinement and they were prepared in identical mould. As recommended by Kenney & Lau (1985), in order to reduce preferential flow, each specimen was wrapped in a latex sleeve, then closed inside the metal mould. The saturation was realized with the same aforementioned method. Finally, all specimens are subjected to a seepage flow in downward direction with deaerated and demineralised water. Three types of hydraulic loading are used: multi-staged hydraulic gradient condition, which consists of increasing the hydraulic gradient by steps, constant hydraulic gradient and flow rate controlled condition



(a)



(b)

Figure 2. Grain size distribution of tested soils, (a) soils KPr25F75, K20L80, DR-C, G3-13, G3-14, C, CH-5, CH-10, (b) soils K10L90, DR-A, DR-B, G3-11, B, KPr20F80.

Table 1. Properties of tested soils.

Tested soils	V_{BS} (-)	ϕ (°)	Finer KL (%)	d_5 (mm)	d_{20} (mm)	d_{50} (mm)	d_{60} (mm)	d_{90} (mm)	P (%)
K10L90	0.581	44	10	0.002	0.162	0.384	0.473	0.693	10
K20L80	1.162	44	20	0.001	0.08	0.315	0.44	0.685	20
B	0.163	44	25	0.111	0.261	2.924	3.25	3.965	1.6
C	0.179	43	27.5	0.109	0.248	2.858	3.217	3.957	1.7
DR-A	0.13	44	20	0.094	0.25	2.412	1.692	2.633	1.7
DR-B	0.163	44	25	0.08	0.151	2.99	2.712	4.727	3.3
DR-C	0.163	44	25	0.08	0.151	2.99	3.671	5.645	3.3
G3-11	0.163	44	25	0.084	0.153	2.924	3.25	3.965	2.7
G3-13	0.098	44	15	0.1	2.127	3.15	3.362	3.993	1.6
G3-14	0.13	44	20	0.094	0.25	3.046	3.309	3.98	1.7
KPr25F75	2.457	37	24.6	0.001	0.009	0.201	0.245	0.411	27
KPr20F80	1.966	37	20	0.0011	0.0295	0.201	0.265	0.422	21.7
CH-5	0.41	49	60	0.094	0.263	0.549	0.75	3.629	3
CH-10	0.291	49	40.5	0.186	0.368	1.381	3.178	8.354	1

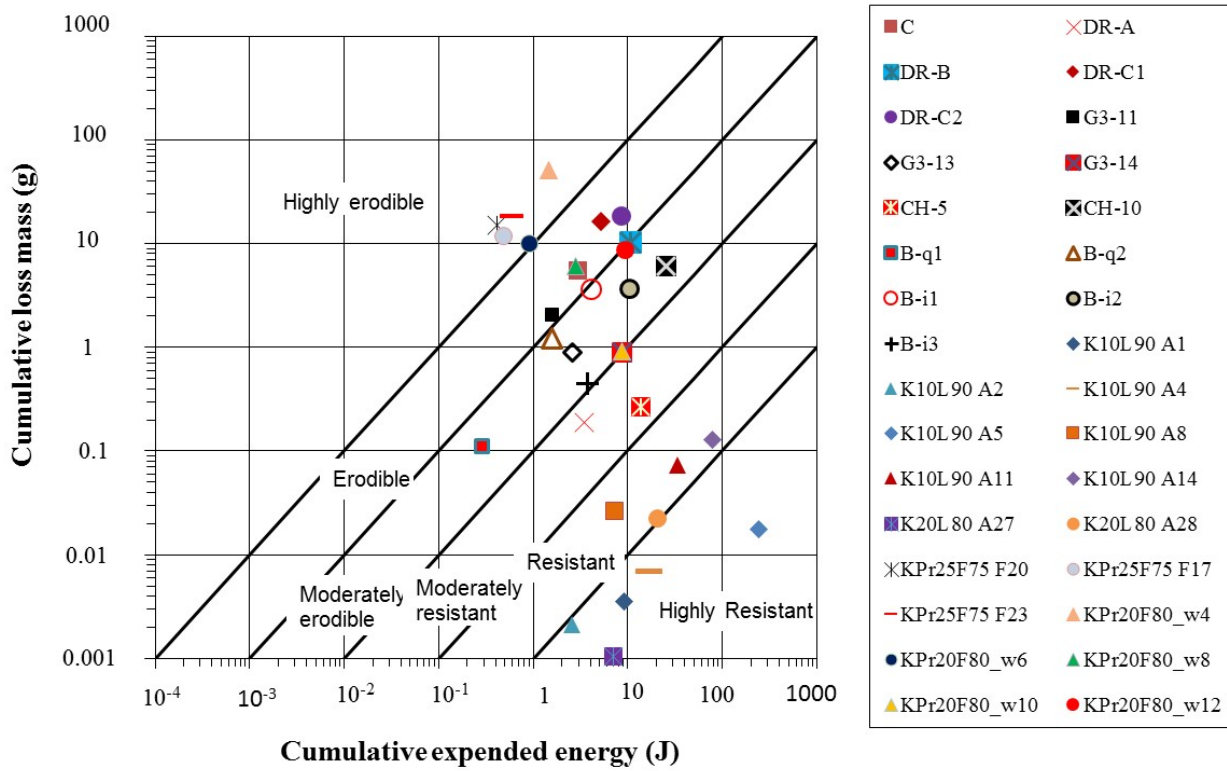


Figure 3. Cumulative eroded dry mass versus cumulative expended energy and suffusion susceptibility categories.

5.4 Suffusion test results

For characterizing the erosion susceptibility, the cumulative expended energy and the corresponding eroded dry mass are determined when hydraulic conductivity becomes constant. The results of all tested specimens are shown on Figure 3 with the corresponding susceptibility categories.

Thanks to the diversity of properties of tested soils, a large range of suffusion susceptibility is obtained. Four specimens are highly resistant (A1, A4, A5, A27), two appear between highly resistant and resistant (A2, A28), three are resistant (A8, A11, A14), CH-5 is moderately resistant, two are between moderately resistant and moderately erodible (G3-14 and KPr20F80_w10), eight are moderately erodible (G3-11, G3-13, CH-10 and B-q1, q2, i1, i2, i3), two are between moderately erodible and erodible (DR-B, KPr20F80_w12), five are erodible (C, DR-A, DR-C1, DR-C2, KPr20F80_w8), KPr20F80_w6 is between erodible and highly erodible, and finally four are highly erodible (KPr25F75 F17, F20, F23, KPr20F80_w4). It is worth noting that for KPr20F80 soil, water content discrepancy of 6% is sufficient to induce a variation of soil erodibility from highly erodible to moderately resistant. This result underlines the influence of the water content at compaction.

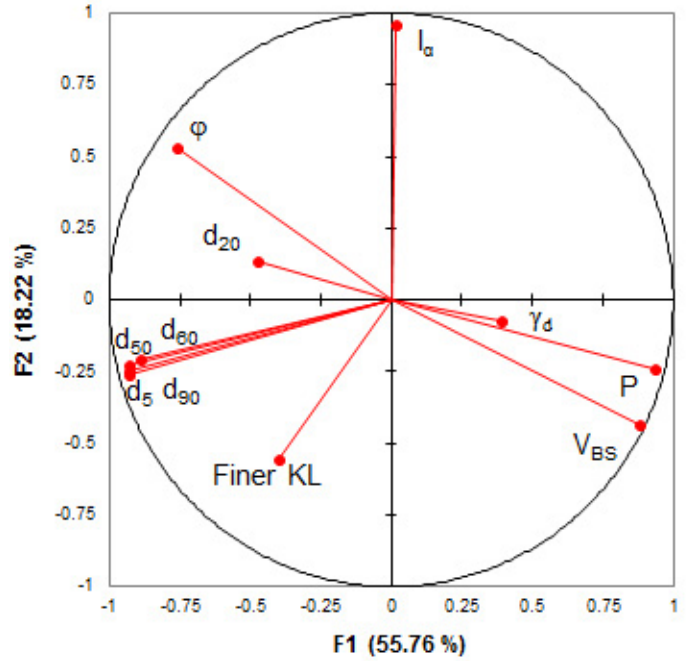
6 RESULTS OF STATISTICAL ANALYSIS

6.1 Results of Principal Component Analysis

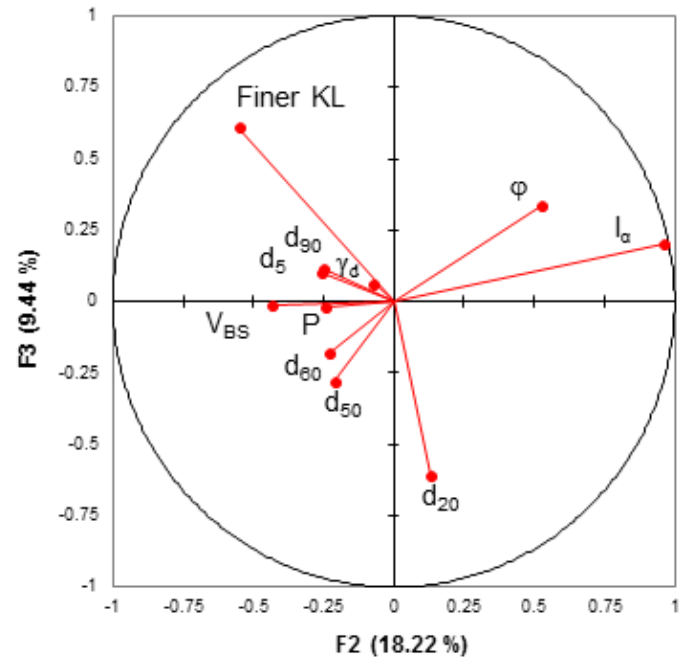
In conformity with the aforementioned identification of predominant parameters, the used physical parameters in this statistical analysis include: the dry unit weight of the soil γ_d , the internal friction angle φ and the blue methylene value V_{BS} . For the characterization of the grain size distribution, five diameters are used: d_5 , d_{20} , d_{50} , d_{60} and d_{90} . These parameters are completed by two distinct percentages: *Finer KL* and *P*.

Figure 4a and 4b show the variables in two first factor planes 1-2 and 2-3 respectively. The principal component analysis of these variables is showed in the correlation circles.

From Fig. (4a) and Fig. (4b), it can be observed that the variables: V_{BS} and *P* or d_5 and d_{90} or d_{50} and d_{60} are close to each other on both two factor planes. It means that they are significantly positively correlated each other. From this analysis, a reduction of the number of physical parameters can be performed.



(a)



(b)

Figure 4. Representation of variables in: (a) factor plane 1-2, (b) factor plane 2-3.

6.2 Multivariate analysis

By leading a new multivariate analysis, eight parameters are kept and a new correlation with erosion resistance index is proposed:

$$I_\alpha = -32.80 + 0.47 \gamma_d + 0.39 V_{BS} + 0.70 \varphi - 0.06 \text{ Finer KL} + 0.04 P - 17.90 d_5 + 0.07 d_{20} + 0.12 d_{50} \quad (3)$$

The obtained correlation coefficient between the prediction and the measurement is $R^2 = 0.93$ for a sample size $N = 32$.

Six parameters (γ_d , V_{BS} , ϕ , P , d_{20} and d_{50}) contribute to equation (3) with the same positive sign. On the contrary, the terms with *Finer KL* and d_5 are negative. Because of the coupling between several parameters, it is difficult to evaluate the contribution of each parameter.

If the gap ratio for a given soil is higher than 1.2, it is assumed gap graded. By distinguishing the gap-graded soils and widely-graded soils, another new correlation is also proposed. For gap-graded soils, the statistical analysis on 22 specimens leads to the following expression:

$$I_a = -20.98 + 0.31 \gamma_d + 5.46 V_{BS} + 0.49 \phi - 0.13 \textit{Finer KL} - 0.16 P \quad (N = 22, R^2 = 0.93) \quad (4)$$

For Widely- graded soils, the new correlation is:

$$I_a = -11.32 + 0.45 \gamma_d + 0.20 V_{BS} + 0.10 \phi + 0.06 \textit{Finer KL} \quad (N = 10, R^2 = 0.93) \quad (5)$$

If we consider the values of parameters and associated factors in equations (4) and (5), it is worth noting the key contribution of the dry unit weight and the internal friction angle.

7 CONCLUSION

A triaxial erodimeter is used to study the suffusion susceptibility of 32 specimens of 14 different soils. Tests realized under different hydraulic loading histories highlight the complexity of suffusion which appears as the result of coupling effect of three processes: detachment, transport and filtration. The interpretation of such tests is based on: the evaluation of the generated load by the fluid flow thanks to the expended energy on one hand, and the cumulative eroded dry mass for the soil response on the other hand. At the end of each test, which corresponds to the invariability of the hydraulic conductivity, the energy based method permits to determine the suffusion susceptibility and the erosion resistance index is computed.

Ten physical parameters were also measured and a statistical analysis is performed in order to identify the main physical parameters for a correlation with the erosion resistance index.

The multivariate statistical analysis leads to an expression of the erosion resistance index as a function of eight physical parameters: initial dry unit weight, blue methylene value, internal friction angle,

percentage of finer based on Kenney and Lau's criteria, percentage finer than 0.063 mm, d_5 , d_{20} and d_{50} .

By distinguishing the gap-graded soils and widely-graded soils, the multivariate statistical analysis leads to an expression of the erosion resistance index as a function of five physical parameters: initial dry unit weight, blue methylene value, internal friction angle, percentage of finer based on Kenney and Lau's criteria and percentage finer than 0.063 mm. Thus, this method allows reducing the number of variables for the description of the suffusion susceptibility.

It is shown that for KPr20F80 soil, water content discrepancy of 6% is sufficient to induce a variation of soil erodibility from highly erodible to moderately resistant. Thus the use of predictive equation for real structure needs to take into account the soil heterogeneities.

8 ACKNOWLEDGEMENT

The authors thank the Ministry of Education and Training of Vietnam, the University of Danang Vietnam, the company IMSRN, the Indonesian Directorate General of Higher Education (DIKTI), the Sultan Agung Islamic University Indonesia, for providing financial support for this work.

REFERENCES

- Arulanandan, K. & Perry, E.B. 1983. Erosion in relation to filter design criteria in earth dams. *Journal of Geotechnical Engineering* 109(5): 682-696.
- Bendahmane, F., Marot, D. & Alexis, A. 2008. Experimental parametric Study of Suffusion and Backward Erosion. *J. Geotech. Geoenviron. Eng.* 134(1): 57-67.
- Chang, D.S. & Zhang, L.M. 2013. Extended internal stability criteria for soils under seepage. *Soils Found.* 53(4): 569-583.
- Fell, R. & Fry, J.J. editors 2007. Internal erosion of dams and their foundations. Taylor & Francis Publisher.
- Fell, R. & Fry, J.J. 2013. Erosion in geomechanics applied to dams and levees. 1-99. Bonelli S. Editor. ISTE – Wiley.
- Garner, S.J. & Fannin, R.J. 2010. Understanding internal erosion: a decade of research following a sinkhole event. *The International J. on Hydropower & Dams* 17: 93-98.
- GTR 1992. Réalisation des remblais et des couches de forme. Guide des Terrassements Routiers, Paris, LCPC, SETRA
- Kenney, T.C. & Lau, D. 1985. Internal stability of granular filters. *Can. Geotech. J.* 22, 215-225.
- Lafleur, J., Mlynarek, J. & Rollin A.L. 1989. Filtration of broadly graded cohesionless soils. *Journal of Geotechnical Engineering* 115(12): 1747-1768.
- Luo, Y.L., Qiao, L., Liu, X.X., Zhan, M.L. & Sheng, J.C. 2013. Hydro-mechanical experiments on suffusion under long-term large hydraulic heads. *Nat. Hazards* 65: 1361-1377.
- Marot, D., Bendahmane, F., Rosquoët, F. & Alexis, A. 2009. Internal flow effects on isotropic confined sand-clay mixtures. *Soil & Sediment Contamination, an International Journal* 18(3): 294-306.

- Marot, D., Bendahmane, F. & Konrad, J.M. 2011a. Multi-channel optical sensor to quantify particle stability under seepage flow. *Can. Geotech. J.* 48: 1772-1787.
- Marot, D., Regazzoni, P.L. & Wahl, T. 2011b. Energy based method for providing soil surface erodibility rankings. *J. Geotech. Geoenviron. Eng.* 137(12): 1290-1294.
- Marot, D., Bendahmane, F. & Nguyen, H.H. 2012. Influence of angularity of coarse fraction grains on internal erosion process. *La Houille Blanche, International Water Journal* 6: 47-53.
- Marot, D., Rochim, A., Nguyen, H.H., Bendahmane, F. & Sibille, L. 2016. Assessing the susceptibility of gap graded soils to internal erosion: proposition of a new experimental methodology. *Natural Hazards*, first online. DOI: 10.1007/s11069-016-2319-8.
- Moffat, R. & Fannin, J. 2006. A large permeameter for study of internal stability in cohesionless soils. *J. ASTM Geotech Test.* 29(4): 273-279.
- Nguyen, H.H., Marot, D. & Bendahmane, F. 2012. Erodibility characterisation for suffusion process in cohesive soil by two types of hydraulic loading. *La Houille Blanche, International Water Journal* 6: 54-60.
- Perzmaier, S. 2007. Hydraulic criteria for internal erosion in cohesionless soil. In *Internal erosion of dams and their Foundations*. Editors R. Fell and J.J. Fry. Taylor & Francis: 179-190.
- Reddi, L.N., Lee, I. & Bonala, M.V.S. 2000. Comparison of internal and surface erosion using flow pump test on a sand-kaolinite mixture. *J. ASTM Geotech Test.* 23(1): 116-122.
- Sibille, L., Lominé, F., Poullain, P., Sail, Y. & Marot, D. 2015. Internal erosion in granular media: direct numerical simulations and energy interpretation. *Hydrol. Processes* 29(9): 2149-2163.
- Skempton, A.W. & Brogan, J.M. 1994. Experiments on piping in sandy gravels. *Géotechnique* 44(3): 440-460.